

Syntheses, Structures, Photoluminescence, and Theoretical Studies of d^{10} Metal Complexes of 2,2'-Dihydroxy-[1,1']binaphthalenyl-3,3'-dicarboxylate

Shao-Liang Zheng,[†] Jin-Hua Yang,[†] Xiao-Lan Yu,[†] Xiao-Ming Chen,^{*†} and Wing-Tak Wong[‡]

School of Chemistry and Chemical Engineering, Sun Yat-Sen University, Guangzhou 510275, China, and Department of Chemistry, The University of Hong Kong, Pokfulam Road, Hong Kong, China

Received July 18, 2003

The free solvated ligand, $H_2bna \cdot CH_3OH \cdot H_2O$ (**1**), and its dimeric complex, $[Cd_2(bna)_2(H_2O)_6]$ (**2**) ($bna = 2,2'$ -dihydroxy-[1,1']-binaphthalene-3,3'-dicarboxylate), were obtained by evaporation of the solutions, while two new d^{10} metal-hydroxy cluster-based coordination polymers, namely $[Cd_8(OH)_4(H_2O)_{10}(bna)_6] \cdot 17H_2O$ (**3**) and $[Hpy]_2[Zn_4(OH)_2(H_2O)_2(bna)_4] \cdot 2H_2O \cdot 2CH_3CN$ (**4**), were obtained by a hydrothermal route. All the compounds have been characterized by X-ray crystallography and photoluminescence measurements. Compound **1** consists of a three-dimensional, hydrogen-bonded supramolecular array, **2** exhibits a dimeric molecule featuring a square motif organized by two Cd(II) atoms and two bna ligands each at the corner, and **3** contains unprecedented $[Cd_8(\mu_3-OH)_2(\mu-OH)_2(\mu-H_2O)_2]^{12+}$ octanuclear metallocrown cores which are interlinked through bna to afford a two-dimensional structure, while **4** features layers with butterfly-shaped $[Zn_4(\mu_3-OH)_2]^{6+}$ clusters. All the complexes display photoluminescent properties in the blue/green range. The manifestation of photoluminescence, as probed by molecular orbital calculations performed on the complexes and also on hypothetical multinuclear complexes, is attributed to a ligand-to-metal charge-transfer mechanism. In addition to presenting a new approach for the study of the photoluminescent properties of metal-cluster-based coordination polymers by using simple model compounds, the study also reveals the dominant role of the structure of the ligand over that of the d^{10} metal-hydroxy (or oxy) cluster and the presence of the cluster significantly increasing the emission lifetime.

Introduction

Metal-organic polymers built from metallic clusters are of current interest because of their interesting molecular topologies and crystal packing motifs as well as the fact that they may be designed with specific functionalities.^{1–6} In addition to being robust and thermally stable, some possess photoluminescent properties, a feature that has contributed to d^{10} metal polynuclear clusters being investigated in the search for new materials.^{5–8} Among the Zn(II) or Cd(II) coordination polymers featuring interesting supramolecular

structures (such as one-dimensional helical ribbons or molecular zippers, two-dimensional molecular square or

* Corresponding author. E-mail: cescxm@zsu.edu.cn. Fax: int code +86 20 8411-2245.

[†] Sun Yat-Sen University.

[‡] The University of Hong Kong.

- (1) Sauvage, J.-P. *Transition Metals in Supramolecular Chemistry*; VCH: Weinheim, 1999 and references cited therein.
- (2) (a) Batten, S. R.; Robson, R. *Angew. Chem., Int. Ed.* **1998**, *37*, 7, 1460–1494. (b) Abourahma, H.; Moulton, B.; Kravtsov, V.; Zaworotko, M. J. *J. Am. Chem. Soc.* **2002**, *124*, 9990–9991.

- (3) (a) Zhang, X. X.; Cui, S. S.-Y.; Williams, I. D. *J. Appl. Phys.* **2000**, *87*, 6007–6009. (b) Tao, J.; Tong, M.-L.; Chen, X.-M. *J. Chem. Soc., Dalton Trans.* **2000**, 3669–3674. (c) Tao, J.; Zhang, X.-M.; Tong, M.-L.; Chen, X.-M. *J. Chem. Soc., Dalton Trans.* **2001**, 770–771. (d) Konar, S.; Mukherjee, P. S.; Zangrando, E.; Lloret, F.; Chaudhuri, N. R. *Angew. Chem., Int. Ed.* **2002**, *41*, 1561–1563. (e) Halder, G. J.; Kepert, C. J.; Moubaraki, B.; Murray, K. S.; Cashion, J. D. *Science* **2002**, *298*, 1762–1765. (f) Lu, J. Y.; Babb, A. M. *Chem. Commun.* **2002**, 1340–1341.
- (4) (a) Li, H.; Eddaoudi, M.; O'Keeffe, O.; Yaghi, O. M. *Nature* **1999**, *402*, 276–279. (b) Chen, B.; Eddaoudi, M.; Hyde, S. T.; O'Keeffe, M.; Yaghi, O. M. *Science* **2001**, *291*, 1021–1023. (c) Eddaoudi, M.; Kim, J.; Rosi, N.; Vodak, D.; Wachter, J.; O'Keeffe, M.; Yaghi, O. M. *Science* **2002**, *295*, 469–472 and references cited therein.
- (5) (a) Weidenbruch, M.; Herrndorf, M.; Schafer, A.; Pohl, S.; Saak, W. *J. Organomet. Chem.* **1989**, *361*, 139–145. (b) Konno, T.; Kageyama, Y.; Okamoto, K. I. *Bull. Chem. Soc. Jpn.* **1994**, *67*, 1957–1960. (c) Lin, W.; Wang, Z.; Ma, L. *J. Am. Chem. Soc.* **1999**, *121*, 11249–11250. (d) Xue, X.; Wang, X.-S.; Wang, L.-Z.; Xiong, R.-G.; Abrahams, B.-F.; You, X.-Z.; Xue, Z.-L.; Che, C.-M. *Inorg. Chem.* **2002**, *41*, 6544–6546.

triangular grids, and interpenetrating/noninterpenetrating three-dimensional networks),^{4–6,9,10} most of them possess photoluminescent properties.^{6,9,10} However, the presence of the polymeric architectures makes such photoluminescent compounds insoluble in common organic solvents^{5b,6,9,10} and renders more detailed analysis of the mechanism of photoluminescence difficult, so that some of the conclusions in the literature may not be reliable.^{9,10}

We have recently reported an organosilver(I) complex with an aromatic carboxylate ligand, H₂bna (bna = 2,2'-dihydroxy-[1,1']-binaphthalene-3,3'-dicarboxylate),¹¹ exhibiting unusual structure and photoluminescence. Meanwhile, it is also known that the photoluminescent properties of the binaphthalene H₂bna compound, whose naphthyl rings are severely twisted across the C–C single bond, are similar to those of another naphthalene derivative, Hna (na = 3-hydroxy-naphthalene-2-carboxylate).¹² As such, the photoluminescence mechanism of the multidimensional Zn(II) or Cd(II) cluster-based coordination polymers of bna is expected to be similar to that of the structurally similar multinuclear complexes of na. On the other hand, it has been shown in previous reports by us¹³ and others¹⁴ that the molecular orbital

(MO) calculations can give a rationalistic understanding of the photoluminescence mechanism. Similarly, we expect that the photoluminescence mechanisms of the multinuclear complexes with bna or na can also be unraveled by MO calculations. In this paper, we describe the preparations, crystal structures, and photoluminescent properties of the free ligand, H₂bna·CH₃OH·H₂O (**1**), and its d^{10} metal complexes, namely [Cd₂(bna)₂(H₂O)₆] (**2**), [Cd₈(OH)₄(H₂O)₁₀(bna)₆]·17H₂O (**3**), and [Hpy]₂[Zn₄(OH)₂(H₂O)₂(bna)₄]·2H₂O·2CH₃CN (**4**) (Hpy = pyridinium).

Experimental Section

Materials and Physical Measurements. The reagents and solvents employed were commercially available and used as received without further purification. The C, H, and N microanalyses were carried out with a Perkin-Elmer 240 elemental analyzer. The FT-IR spectra were recorded from KBr pellets in the range 4000–400 cm⁻¹ on a Bio-Rad FTS-7 spectrometer. The emission/excitation spectra were recorded on a Perkin-Elmer LS50B fluorescence spectrophotometer. The time-resolved single-photon absorption fluorescence for **1** and **2** was measured with a third harmonic of a mode-locked Nd:YAG laser (Continuum PY61C-10) with a duration of 60 ps used as the excitation source, with a streak camera (Hamamatsu Model C1587, 6 ps resolution) as a recorder. For **3–4**, the third harmonics, 355 nm line of an Nd:YAG laser (Quantel Brilliant B) with a duration of 10 ns, was used as the excitation source.

Synthesis. H₂bna·CH₃OH·H₂O (1**).** The crystals of **1** were obtained (yield 78%) by slow diffusion of diethyl ether into a methanol solution of the pale-yellow sample, which was prepared by the hydrolytic reaction of its dimethyl ester.¹⁵ Elemental analysis calcd (%) for C₂₃H₂₀O₈ **1**: C, 65.09; H, 4.75. Found: C, 65.11; H, 4.73. IR data (KBr, cm⁻¹): 3436s, br, 1609m, 1571vs, 1500m, 1439vs, 1398s, 1348m, 1246m, 1130w, 1087m, 1006w, 930w, 813m, 755m, 630w, 541m, 439w.

[Cd₂(bna)₂(H₂O)₆] (2**).** A solution (5 mL) of H₂bna (0.187 g, 0.5 mmol) was added dropwise to a stirred methanol solution (5 mL) of Cd(NO₃)₂·4H₂O (0.154 g, 0.5 mmol) at 50 °C for 30 min. The resulting pale-yellow solution was allowed to stand in air at room temperature for two weeks, yielding pale-yellow crystals in good yield (37%). Elemental analysis calcd (%) for C₄₄H₃₆Cd₂O₁₈ **2**: C, 49.04; H, 3.37. Found: C, 49.02; H 3.32. IR data (KBr, cm⁻¹): 3472s, br, 1637m, 1560s, 1558vs, 1503m, 1460vs, 1398m, 1369vs, 1342m, 1238m, 1130w, 1016w, 942m, 876m, 809m, 755m, 630w, 597m, 440w.

[Cd₈(OH)₄(H₂O)₁₀(bna)₆]·17H₂O (3**).** An MeCN–H₂O [1:4 (v/v), 10 mL] solution containing Cd(NO₃)₂·4H₂O (0.154 g, 0.5 mmol) and H₂bna (0.187 g, 0.5 mmol) was stirred for 20 min in air, and then placed in Parr Teflon-lined stainless steel vessel (23 mL). After addition of triethylamine (0.7 mL, 5 mmol), the vessel was sealed and heated at 160 °C for 120 h, cooled to 100 °C at a rate of 5 °C h⁻¹, and held for 10 h, followed by further cooling to room temperature. Pale-yellow crystals of **3** were collected, washed with water, and dried in air (yield 42%). Elemental analysis calcd (%) for C₁₃₂H₁₃₀Cd₈O₆₇ **3**: C, 42.99; H, 3.55. Found: C, 43.02; H, 3.52. IR data (KBr, cm⁻¹): 3452m, br, 1725m, 1619m, 1552vs, 1505m, 1459m, 1401vs, 1370s, 1348s, 1241m, 1153m, 1098m, 1077m, 1003w, 943m, 879m, 809m, 750m, 623w, 564w, 529m, 482w, 439w.

- (6) (a) Tao, J.; Tong, M.-L.; Shi, J.-X.; Chen, X.-M.; Ng, S. W. *Chem. Commun.* **2000**, 2043–2044. (b) Tao, J.; Shi, J.-X.; Tong, M.-L.; Zhang, X.-X.; Chen, X.-M. *Inorg. Chem.* **2001**, *40*, 6328–6330. (c) Tao, J.; Yin, X.; Jiang, Y.-B.; Yang, L.-F.; Huang, R.-B.; Zheng, L.-S. *Eur. J. Inorg. Chem.* **2003**, 2678–2682.
- (7) (a) Hiltunen, L.; Leskelä, M.; Niinistö, L. *Acta Chem. Scand., Ser. A* **1987**, *41*, 548–555. (b) Kunkely, H.; Vogler, A. *J. Chem. Soc., Chem. Commun.* **1990**, 1204–1205. (c) Bertocello, R.; Betinelli, M.; Casarin, M.; Gulino, A.; Tondello, E.; Vittadini, A. *Inorg. Chem.* **1992**, *31*, 1558–1565.
- (8) (a) Lee, C.-F.; Chin, K.-F.; Peng, S.-M.; Che, C.-M. *J. Chem. Soc., Dalton Trans.* **1993**, 467–470. (b) Ho, K.-Y.; Yu, W.-Y.; Cheung, K.-K.; Che, C.-M. *Chem. Commun.* **1998**, 2491–2492.
- (9) (a) Dai, J.-C.; Wu, X.-T.; Fu, Z.-Y.; Cui, C.-P.; Wu, S.-M.; Du, W.-X.; Wu, L.-M.; Zhang, H.-H.; Sun, R.-Q. *Inorg. Chem.* **2002**, *41*, 1391–1396. (b) Chen, W.; Wang, J.-Y.; Chen, C.; Yue, Q.; Yuan, H.-M.; Chen, J.-S.; Wang, S.-N. *Inorg. Chem.* **2003**, *42*, 944–946. (c) Long, L.-S.; Ren, Y.-P.; Ma, L.-H.; Jiang, Y.-B.; Huang, R.-B.; Zheng, L.-S. *Inorg. Chem. Commun.* **2003**, *6*, 690–693. (d) Luo, J.-H.; Hong, M.-C.; Wang, R.-H.; Cao, R.; Han, L.; Lin, Z.-Z. *Eur. J. Inorg. Chem.* **2003**, 2705–2710. (e) Zhang, L.-Y.; Liu, G.-F.; Zheng, S.-L.; Ye, B.-H.; Zhang, X.-M.; Chen, X.-M. *Eur. J. Inorg. Chem.* **2003**, 2965–2971.
- (10) (a) Chen, Z.-F.; Xiong, R.-G.; Zhang, J.; Zuo, J.-L.; You, X.-Z.; Che, C.-M.; Fun, H.-K. *J. Chem. Soc., Dalton Trans.* **2000**, 4010–4012. (b) Xiong, R.-G.; Zuo, J.-L.; You, X.-Z.; Abrahams, B. F.; Bai, Z.-P.; Che, C.-M.; Fun, H.-K. *Chem. Commun.* **2000**, 2061–2062. (c) Chen, Z.-F.; Xiong, R.-G.; Zhang, J.; Chen, X.-T.; Xue, Z.-L.; You, X.-Z. *Inorg. Chem.* **2001**, *40*, 4075–4077. (d) Long, L.-S.; Ren, Y.-P.; Ma, L.-H.; Jiang, Y.-B.; Huang, R.-B.; Zheng, L.-S. *Inorg. Chem. Commun.* **2003**, *6*, 690–693. (e) Zhang, J.; Xie, Y.-R.; Ye, Q.; Xiong, R.-G.; Xue, Z.-L.; You, X. *Z. Eur. J. Inorg. Chem.* **2003**, 2572–2577. (f) Wang, S.-T.; Hou, Y.; Wang, E.-B.; Li, Y.-G.; Xu, L.; Peng, J.; Liu, S.-X.; Hu, C.-W. *New J. Chem.* **2003**, 1144–1147.
- (11) Zheng, S.-L.; Tong, M.-L.; Tan, S.-D.; Wang, Y.; Shi, J.-X.; Tong, Y.-X.; Lee, H.-K.; Chen, X.-M. *Organometallics* **2001**, *20*, 5319–5325.
- (12) Valeur, B. *Molecular Fluorescence: Principles and Applications*; Wiley-VCH: Weinheim, 2002.
- (13) Zheng, S.-L.; Zhang, J.-P.; Chen, X.-M.; Huang, Z.-L.; Lin, Z.-Y.; Wong, W.-T. *Chem.-Eur. J.* **2003**, *9*, 3888–3896.
- (14) (a) Burrows, P. E.; Shen, Z.; Bulovic, V.; McCarty, D. M.; Forrest, S. R.; Cronin, J. A.; Thompson, M. E. *J. Appl. Phys.* **1996**, *79*, 7991–8006. (b) Ashenurst, J.; Brancaleon, L.; Hassan, A.; Liu, W.; Schmider, H.; Wang, S.; Wu, Q. *Organometallics* **1998**, *17*, 3186–3195. (c) Yang, W. Y.; Schmider, H.; Wu, Q.; Zhang, Y. S.; Wang, S. *Inorg. Chem.* **2000**, *39*, 2397–2404. (d) Liu, S.-F.; Wu, Q.; Schmider, H. L.; Aziz, H.; Hu, N.-X.; Popovic, Z.; Wang, S. *J. Am. Chem. Soc.* **2000**, *122*, 3671–3678.

(15) Martin, H.; Jiri, Z. *Org. Prep. Proced. Int.* **1991**, *23*, 200–203.

Table 1. Crystal Data and Structure Refinements for **1–4**

chemical formula	C ₂₃ H ₂₀ O ₈	C ₄₄ H ₃₆ - Cd ₈ O ₁₈	C ₁₃₂ H ₁₃₀ - Cd ₈ O ₆₇	C ₁₀₂ H ₇₆ N ₄ - O ₃₀ Zn ₄
<i>a</i> /Å	15.368(2)	15.822(8)	13.169(1)	13.795(5)
<i>b</i> /Å	7.1578(9)	9.162(3)	16.736(1)	14.348(7)
<i>c</i> /Å	19.165(3)	15.345(4)	17.314(1)	15.220(8)
α /deg	90	90	113.416(3)	109.84(7)
β /deg	106.310(2)	90.49(1)	100.613(3)	94.01(7)
γ /deg	90	90	93.647(3)	110.34(6)
<i>V</i> /Å ³	2023.3(5)	2224(2)	3401.9(5)	2596(2)
<i>Z</i>	4	2	1	1
<i>fw</i>	424.39	1077.53	3687.56	2099.15
space group	<i>P</i> 2 ₁ / <i>n</i> (No. 14)	<i>P</i> 2 ₁ / <i>c</i> (No. 14)	<i>P</i> 1̄ (No. 2)	<i>P</i> 1̄ (No. 2)
<i>T</i> (K)	293(2)	293(2)	293(2)	293(2)
λ (Mo K α) (Å)	0.71073	0.71073	0.71073	0.71073
ρ_{calcd} /g cm ⁻³	1.393	1.609	1.800	1.343
μ (Mo K α)/ mm ⁻¹	0.106	1.032	1.329	0.990
R1 ^a [<i>I</i> > 2 σ (<i>I</i>)]	0.0540	0.0495	0.0477	0.0698
wR2 ^a	0.1778	0.1271	0.1292	0.2154

$$^a R1 = \sum |F_o| - |F_c| / \sum |F_o|, wR2 = [\sum w(F_o^2 - F_c^2)^2 / \sum w(F_o^2)]^{1/2}.$$

[Hpy]₂[Zn₄(OH)₂(H₂O)₂(bna)₄]·2H₂O·2CH₃CN (**4**). An MeCN–H₂O [1:4 (v/v); 10 mL] solution containing Zn(NO₃)₂·6H₂O (0.158 g, 0.5 mmol) and H₂bna (0.187 g, 0.5 mmol) was stirred for 20 min in air, and then placed in a Parr Teflon-lined stainless steel vessel (23 mL). After addition of pyridine (1 mL), the vessel was sealed and heated at 160 °C for 120 h, cooled to 100 °C at a rate of 5 °C h⁻¹, and held for 10 h, followed by further cooling to room temperature. Pale-yellow crystals of **4** were collected, washed with water, and dried in air (yield 42%). Elemental analysis calcd (%) for C₁₀₂H₇₆N₄O₃₀Zn₄ **4**: C, 58.36; H, 3.65; N, 2.67. Found: C, 58.40; H, 3.62; N, 2.65. IR data (KBr, cm⁻¹): 3446m, br, 2230s, 1645m, 1570s, 1562vs, 1509m, 1439s, 1385vs, 1341m, 1239m, 1130w, 1008w, 930w, 808m, 748m, 671m, 619w, 535m, 478m, 442w, 423w.

X-ray Crystallography. Structure diffraction intensities for **1** and **3** were collected at 293 K on a Bruker Smart Apex CCD area-detector diffractometer (Mo K α , $\lambda = 0.71073$ Å), while **2** and **4** were collected on a Siemens *R3m* diffractometer using the ω -scan technique with graphite-monochromated Mo K α ($\lambda = 0.71073$ Å) radiation. Lorentz-polarization and absorption corrections were applied for the four compounds.^{16,17} The structures were solved with direct methods and refined with full-matrix least-squares technique using the SHELXS-97 and SHELXL-97 programs, respectively.^{18,19} Anisotropic displacement parameters were applied to all non-hydrogen atoms. The organic hydrogen atoms were generated geometrically (C–H 0.96 Å); the aqua hydrogen atoms were located from difference maps and refined with isotropic displacement parameters. Analytical expressions of neutral-atom scattering factors were employed, and anomalous dispersion corrections were incorporated.²⁰ Crystal data as well as details of data collection and refinement for the complexes are summarized in Table 1. Selected bond distances and bond angles are listed in Table 2. Drawings were produced with SHELXTL.²¹ CCDC files contain supplementary crystallographic data for this paper. These data can be obtained

(16) Blessing, R. *Acta Crystallogr., Sect. A* **1995**, *51*, 33–38.

(17) North, A. C. T.; Phillips, D. C.; Mathews, F. S. *Acta Crystallogr., Sect. A* **1968**, *24*, 351–359.

(18) Sheldrick, G. M. *SHELXS-97, Program for Crystal Structure Solution*; Göttingen University: Göttingen, Germany, 1997.

(19) Sheldrick, G. M. *SHELXL-97, Program for Crystal Structure Refinement*; Göttingen University: Göttingen, Germany, 1997.

(20) Cromer, T. *International Tables for X-ray Crystallography*, Kluwer Academic Publisher: Dordrecht, 1992; Vol. C, Tables 4.2.6.8 and 6.1.1.4.

(21) Sheldrick, G. M. *SHELXTL*, Version 5; Siemens Industrial Automation Inc.: Madison, WI, 1995.

free of charge via www.ccdc.cam.ac.uk/conts/retrieving.html (or from the Cambridge Crystallographic Data Center, 12 Union Road, Cambridge CB2 1EZ, U.K. Fax: (+44) 1223-336-033. E-mail: deposit@ccdc.cam.ac.uk).

Calculation Details. Density functional calculations were performed, employing the Gaussian98 suite of programs,²² at the B3LYP level. The basis set used for C, O, N, and H atoms was 6-31G while effective core potentials with a LanL2DZ basis set were employed for transition metals. The contour plots of MOs were obtained with the Molden 3.5 graphic program.²³

Results and Discussion

Syntheses and Characterization. The hydrothermal method has been proven to be very effective for the syntheses of zeolites, nanomaterials, and, more recently, coordination polymers. It is well-known that small changes in one or more of hydrothermal parameters, such as the temperature, reaction time, pH value, and molar ratio of the reactants, may exert profound influence on final reaction products. During the past few years, we have explored the synthesis of metal-cluster-based coordination polymers containing mixed organic ligands under typical hydrothermal conditions (i.e., 120–180 °C and 2–7 days) and found that pH values of 7–8 are most suitable in the formation of metal–hydroxy (or oxy) clusters.⁶ This pH condition was used in the preparation of **3** and **4**; at this pH, the metal–hydroxy clusters result from the hydrolysis of metal ions. The formation of clusters is avoided by merely carrying out the reaction in water; **2** was isolated from an open solution of cadmium nitrate and the acid. It should also be pointed out that the reaction conditions employed in this work were found to be appropriate for isolation of good-quality crystals as the products.

In general, the IR spectra show features attributable to the carboxylate stretching vibrations of the complexes. For **2**, differences (Δ) between the antisymmetric stretching and symmetric stretching bands of the carboxylate groups are 100 and 189 cm⁻¹, attributable to the monodentate mode and chelating mode of the carboxylate groups, respectively (Scheme 1a). For **3**, only one Δ value of 151 cm⁻¹ assignable to the bis-bidentate mode of the carboxylate groups (Scheme 1b) is found, whereas for **4**, two Δ values of 131 and 177 cm⁻¹ are found, being attributable to the monodentate and bis-bidentate mode of the carboxylate groups, respectively (Scheme 1b,c). The different Δ values in **2–4** indicate that the carboxylate group function in different coordination

- (22) Frisch, M. J.; Trucks, G. W.; Schlegel, H. B.; Scuseria, G. E.; Robb, M. A.; Cheeseman, J. R.; Zakrzewski, V. G.; Montgomery, J. A., Jr.; Stratmann, R. E.; Burant, J. C.; Dapprich, S.; Millam, J. M.; Daniels, A. D.; Kudin, K. N.; Strain, M. C.; Farkas, O.; Tomasi, J.; Barone, V.; Cossi, M.; Cammi, R.; Mennucci, B.; Pomelli, C.; Adamo, C.; Clifford, S.; Ochterski, J.; Petersson, G. A.; Ayala, P. Y.; Cui, Q.; Morokuma, K.; Malick, D. K.; Rabuck, A. D.; Raghavachari, K.; Foresman, J. B.; Cioslowski, J.; Ortiz, J. V.; Stefanov, B. B.; Liu, G.; Liashenko, A.; Piskorz, P.; Komaromi, I.; Gomperts, R.; Martin, R. L.; Fox, D. J.; Keith, T.; Al-Laham, M. A.; Peng, C. Y.; Nanayakkara, A.; Gonzalez, C.; Challacombe, M.; Gill, P. M. W.; Johnson, B. G.; Chen, W.; Wong, M. W.; Andres, J. L.; Head-Gordon, M.; Replogle, E. S.; Pople, J. A. *Gaussian 98*, revision A.5; Gaussian, Inc.: Pittsburgh, PA, 1998.
- (23) Schaftenaar, G. *Molden*, Version 3.5; CAOS/CAMM Center Nijmegen, Toernooiveld: Nijmegen, Netherlands, 1999.

Table 2. Bond Lengths (Å) and Angles (deg) for **1–4**^a

				Compound 1			
O(1)···O(7)		2.614(3)		O(5)···O(6)		2.611(2)	
O(2)···O(3)		2.544(2)		O(1W)···O(5b)		2.823(3)	
O(3)···O(1W)		2.830(2)		O(7)···O(4c)		3.145(3)	
O(4)···O(1Wa)		2.562(2)					
				Complex 2			
Cd(1)–O(2W)	2.290(4)	O(2W)···O(4c)	3.130(6)	O(2W)–Cd(1)–O(1W)	93.9(2)	O(5a)–Cd(1)–O(1)	91.4(1)
Cd(1)–O(1W)	2.327(5)	O(3W)···O(4a)	2.742(5)	O(2W)–Cd(1)–O(5a)	171.4(1)	O(3W)–Cd(1)–O(1)	83.4(1)
Cd(1)–O(5a)	2.342(3)	O(3W)···O(6d)	2.936(5)	O(1W)–Cd(1)–O(5a)	82.1(2)	O(2W)–Cd(1)–O(2)	107.7(2)
Cd(1)–O(3W)	2.388(3)	O(2)···O(3)	2.605(4)	O(2W)–Cd(1)–O(3W)	91.2(2)	O(1W)–Cd(1)–O(2)	108.4(1)
Cd(1)–O(1)	2.405(4)	O(3)···O(4e)	3.015(5)	O(1W)–Cd(1)–O(3W)	111.2(1)	O(5a)–Cd(1)–O(2)	80.8(1)
Cd(1)–O(2)	2.420(3)	O(5)···O(6)	2.557(5)	O(5a)–Cd(1)–O(3W)	83.3(1)	O(3W)–Cd(1)–O(2)	134.5(1)
O(1W)···O(3Wb)	3.074(5)			O(2W)–Cd(1)–O(1)	94.4(2)	O(1)–Cd(1)–O(2)	54.9(1)
				O(1W)–Cd(1)–O(1)	163.0(1)		
				Complex 3			
Cd(1)–O(16a)	2.218(4)	O(14)···O(15)	2.508(5)	O(16a)–Cd(1)–O(13)	93.8(1)	O(17a)–Cd(3)–O(2W)	166.3(2)
Cd(1)–O(13)	2.262(4)	O(17)···O(18)	2.554(6)	O(16a)–Cd(1)–O(2H)	97.5(1)	O(2H)–Cd(3)–O(2W)	99.8(2)
Cd(1)–O(2H)	2.276(4)	O(3)···O(10W)	2.94(1)	O(13)–Cd(1)–O(2H)	162.4(1)	O(5)–Cd(3)–O(2W)	84.1(2)
Cd(1)–O(4)	2.311(4)	O(3)···O(6W)	3.122(7)	O(16a)–Cd(1)–O(4)	93.0(2)	O(17a)–Cd(3)–O(1Hc)	89.6(2)
Cd(1)–O(1W)	2.314(4)	O(4)···O(13W)	2.82(2)	O(13)–Cd(1)–O(4)	84.2(2)	O(2H)–Cd(3)–O(1Hc)	87.2(1)
Cd(1)–O(7)	2.339(4)	O(6)···O(6W)	2.941(7)	O(2H)–Cd(1)–O(4)	81.8(2)	O(5)–Cd(3)–O(1Hc)	171.3(1)
Cd(2)–O(1H)	2.177(3)	O(12)···O(9W)	2.93(1)	O(16a)–Cd(1)–O(1W)	167.5(2)	O(2W)–Cd(3)–O(1Hc)	87.2(2)
Cd(2)–O(14)	2.182(4)	O(18)···O(8W)	2.97(1)	O(13)–Cd(1)–O(1W)	86.7(1)	O(17a)–Cd(3)–O(10d)	80.9(2)
Cd(2)–O(8)	2.224(4)	O(1H)···O(8Wf)	3.12(1)	O(2H)–Cd(1)–O(1W)	85.1(1)	O(2H)–Cd(3)–O(10d)	164.0(2)
Cd(2)–O(1b)	2.241(4)	O(1W)···O(2Hc)	2.448(5)	O(4)–Cd(1)–O(1W)	99.5(2)	O(5)–Cd(3)–O(10d)	101.8(2)
Cd(2)–O(1W)	2.357(4)	O(1W)···O(7W)	2.62(2)	O(16a)–Cd(1)–O(7)	82.4(2)	O(2W)–Cd(3)–O(10d)	85.4(2)
Cd(3)–O(17a)	2.218(4)	O(2W)···O(9Wc)	2.97(1)	O(13)–Cd(1)–O(7)	98.7(1)	O(1Hc)–Cd(3)–O(10d)	77.9(2)
Cd(3)–O(2H)	2.272(4)	O(3W)···O(11W)	2.57(2)	O(2H)–Cd(1)–O(7)	96.1(2)	O(1H)–Cd(4)–O(11e)	118.7(2)
Cd(3)–O(5)	2.295(4)	O(4W)···O(8Wf)	3.11(2)	O(4)–Cd(1)–O(7)	174.7(2)	O(1H)–Cd(4)–O(4W)	100.3(3)
Cd(3)–O(2W)	2.301(5)	O(5W)···O(12W)	2.90(2)	O(1W)–Cd(1)–O(7)	85.2(2)	O(11e)–Cd(4)–O(4W)	92.8(3)
Cd(3)–O(1Hc)	2.340(3)	O(6W)···O(9d)	2.891(7)	O(1H)–Cd(2)–O(14)	119.1(1)	O(1H)–Cd(4)–O(2b)	89.8(2)
Cd(3)–O(10d)	2.353(4)	O(6W)···O(14W)	2.96(2)	O(1H)–Cd(2)–O(8)	116.9(2)	O(11e)–Cd(4)–O(2b)	89.0(2)
Cd(4)–O(1H)	2.242(3)	O(7W)···O(11Wf)	2.70(3)	O(14)–Cd(2)–O(8)	123.3(2)	O(4W)–Cd(4)–O(2b)	167.3(3)
Cd(4)–O(11e)	2.256(5)	O(7W)···O(8Wf)	2.86(2)	O(1H)–Cd(2)–O(1b)	107.2(1)	O(1H)–Cd(4)–O(3W)	81.1(2)
Cd(4)–O(4W)	2.280(7)	O(7W)···O(7c)	2.94(2)	O(14)–Cd(2)–O(1b)	90.3(2)	O(11e)–Cd(4)–O(3W)	160.2(2)
Cd(4)–O(2b)	2.290(4)	O(8W)···O(11Wf)	2.63(2)	O(8)–Cd(2)–O(1b)	81.5(2)	O(4W)–Cd(4)–O(3W)	82.7(3)
Cd(4)–O(3W)	2.388(6)	O(8W)···O(11W)	2.77(2)	O(1H)–Cd(2)–O(1W)	87.9(1)	O(2b)–Cd(4)–O(3W)	91.4(2)
Cd(4)–O(5W)	2.404(7)	O(9W)···O(12Wa)	2.68(2)	O(14)–Cd(2)–O(1W)	84.7(1)	O(1H)–Cd(4)–O(5W)	160.5(2)
O(2)···O(3)	2.553(6)	O(11W)···O(11Wf)	3.04(3)	O(8)–Cd(2)–O(1W)	89.2(2)	O(11e)–Cd(4)–O(5W)	80.1(3)
O(5)···O(6)	2.558(5)	O(12W)···O(13Wf)	2.51(2)	O(1b)–Cd(2)–O(1W)	164.6(2)	O(4W)–Cd(4)–O(5W)	82.7(4)
O(8)···O(9)	2.524(5)	O(13W)···O(11Wf)	2.73(2)	O(17a)–Cd(3)–O(2H)	93.4(2)	O(2b)–Cd(4)–O(5W)	85.3(3)
O(11)···O(12)	2.563(6)	O(14W)···O(14Wg)	2.97(4)	O(17a)–Cd(3)–O(5)	99.0(2)	O(3W)–Cd(4)–O(5W)	80.2(3)
				O(2H)–Cd(3)–O(5)	93.8(1)		
				Complex 4			
Zn(1)–O(1H)	2.077(4)	Zn(2)–O(1Hc)	2.182(5)	O(1H)–Zn(1)–O(2)	95.3(2)	O(10a)–Zn(1)–O(1W)	92.1(2)
Zn(1)–O(2)	2.097(5)	O(1H)···N(2d)	3.28(2)	O(1H)–Zn(1)–O(8)	91.1(2)	O(5b)–Zn(1)–O(1W)	173.6(2)
Zn(1)–O(8)	2.102(5)	O(1W)···O(11a)	2.651(8)	O(8)–Zn(1)–O(2)	173.4(2)	O(1c)–Zn(2)–O(4b)	106.9(2)
Zn(1)–O(10a)	2.106(4)	O(1W)···O(2Wc)	2.736(6)	O(1H)–Zn(1)–O(10a)	178.1(2)	O(1c)–Zn(2)–O(1H)	137.1(2)
Zn(1)–O(5b)	2.197(5)	O(3)···O(2)	2.640(6)	O(2)–Zn(1)–O(10a)	85.9(2)	O(4b)–Zn(2)–O(1H)	115.9(2)
Zn(1)–O(1W)	2.208(6)	O(6)···O(5)	2.624(6)	O(8)–Zn(1)–O(10a)	87.8(2)	O(1c)–Zn(2)–O(7)	86.0(2)
Zn(2)–O(1c)	1.981(4)	O(9)···O(8)	2.576(7)	O(1H)–Zn(1)–O(5b)	97.0(2)	O(4b)–Zn(2)–O(7)	95.5(2)
Zn(2)–O(4b)	2.026(4)	O(12)···O(11)	2.552(8)	O(2)–Zn(1)–O(5b)	88.3(2)	O(1H)–Zn(2)–O(7)	93.1(2)
Zn(2)–O(1H)	2.020(5)	O(2W)···O(4d)	3.038(1)	O(8)–Zn(1)–O(5b)	92.4(2)	O(1c)–Zn(2)–O(1Hc)	96.9(2)
Zn(2)–O(7)	2.128(5)			O(10a)–Zn(1)–O(5b)	81.6(2)	O(4b)–Zn(2)–O(1Hc)	89.5(2)
				O(1H)–Zn(1)–O(1W)	89.4(2)	O(1H)–Zn(2)–O(1Hc)	80.8(2)
				O(2)–Zn(1)–O(1W)	89.9(3)	O(7)–Zn(2)–O(1Hc)	173.3(2)
				O(8)–Zn(1)–O(1W)	88.7(3)		

^a Symmetry codes: (a) $-x, -y, -z$; (b) $x, y - 1, z$; (c) $x + 1/2, -y - 1/2, z - 1/2$ for **1**; (a) $-x, -y, -z$; (b) $-x, -y, -z + 1$; (c) $x, y, z + 1$; (d) $x, -y - 1/2, z + 1/2$; (e) $x, -y + 1/2, z + 1/2$ for **2**; (a) $x - 1, y, z$; (b) $x, y - 1, z$; (c) $-x + 1, -y + 1, -z + 1$; (d) $x, y + 1, z$; (e) $-x + 1, -y, -z + 1$; (f) $-x + 2, -y + 1, -z + 1$; (g) $-x + 1, -y + 2, -z + 1$ for **3**; (a) $-x + 1, -y + 2, -z + 2$; (b) $-x + 1, -y + 1, -z + 1$; (c) $-x, -y + 1, -z + 1$; (d) $x - 1, y, z$ for **4**.

fashions (Scheme 1),²⁴ in agreement with the crystal structures.

Crystal Structures. Compound **1** consists of H₂bna, methanol, and water molecules. The two naphthyl rings in

H₂bna are twisted at 78.4°. A pair of H₂bna, each using the same carboxylic oxygen atoms, forms two donor hydrogen bonds [O(4)···O(1Wa) 2.562(2) Å] and two acceptor hydrogen bonds [O(1W)···O(5b) 2.823(3) Å] with a pair of water molecules as described by the graph set of R₄⁴(12).²⁵ Each water molecule further forms a donor hydrogen bond

(24) (a) Nakamoto, K. *Infrared and Raman Spectra of Inorganic and Coordination Compounds*; John Wiley & Sons: New York, 1986. (b) Zheng, S.-L.; Tong, M.-L.; Chen, X.-M. *J. Chem. Soc., Dalton Trans.* **2001**, 586–592.

(25) Etter, M. C. *Chem. Res.* **1990**, 23, 120–126.

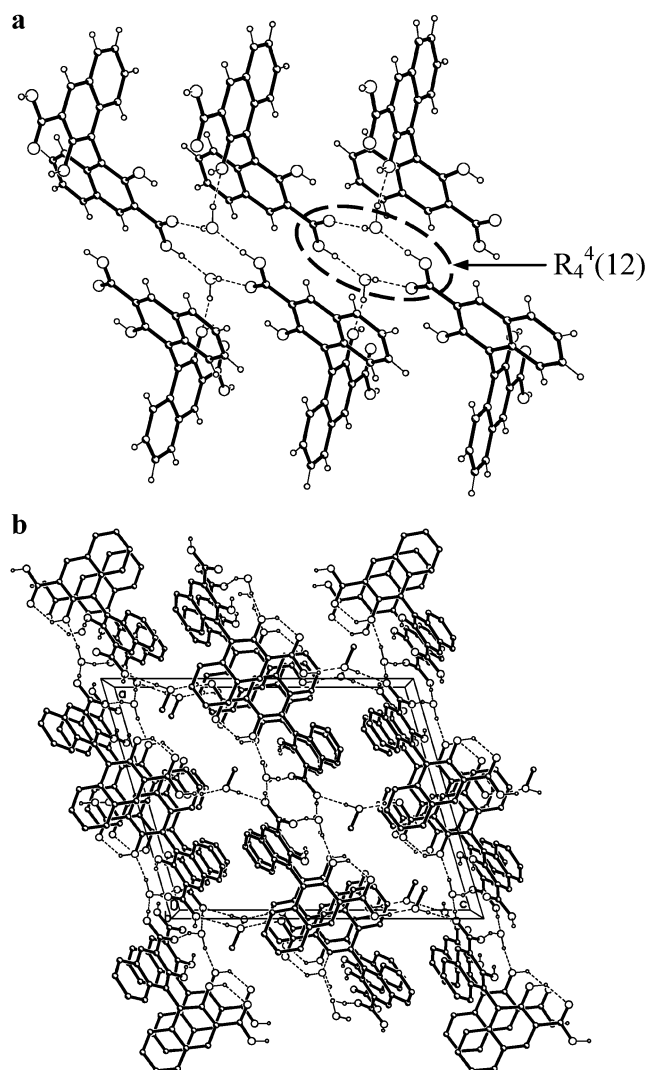
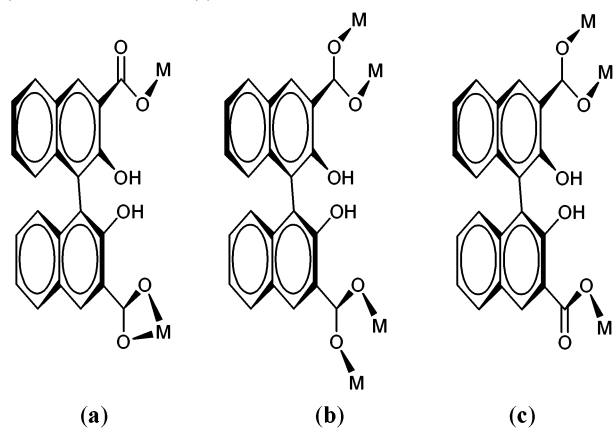


Figure 1. Perspective views showing the one-dimensional hydrogen-bonded chain featuring a graph set of $R_4^4(12)$ (a) and three-dimensional supramolecular array viewed along the b -axis direction (b) in **1**.

Scheme 1. The Coordination Mode of bna (a) Monodentate-Chelating, (b) Bis-Bidentate, and (c) Monodentate-Bidentate



with the hydroxyl oxygen of adjacent naphthyl ring from another H_2bna , resulting in a one-dimensional hydrogen-bonded chain (Figure 1a). Adjacent hydrogen-bonded chains are stacked through offset π - π aromatic stacking interactions with the face-to-face distance of ca. 3.47 Å, furnishing two-dimensional layers along the (011) plane. The layers are

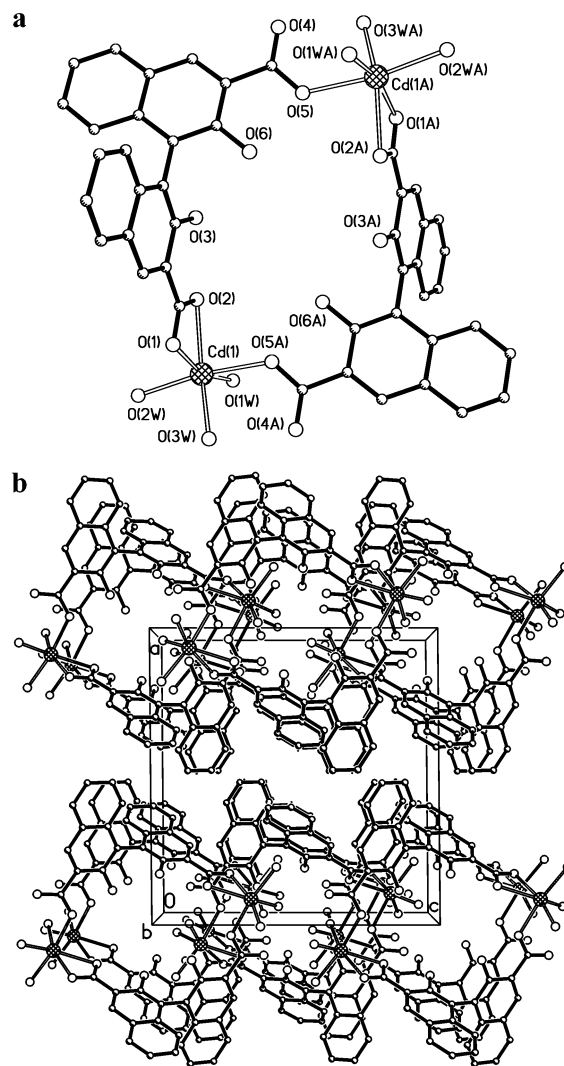


Figure 2. Perspective views showing the dimeric structure (a) and three-dimensional supramolecular array viewed along the b -axis direction (b) in **2**.

further extended into a three-dimensional supramolecular array via the methanol molecules which form the donor [O(7)⋯O(4c) 3.145(3) Å] and acceptor [O(1)⋯O(7) 2.614(3) Å] hydrogen bonds with the oxygen atoms from different carboxylic groups (Figure 1b).

Complex **2** features a square motif formed by two Cd(II) atoms and two bna ligands each at the corner. As shown in Figure 2a, each Cd(II) atom exists in a distorted octahedral geometry, being ligated by two carboxylate oxygen atoms [Cd(1)–O 2.405(4) and 2.420(3) Å] from a bna, and another carboxylate oxygen atom [Cd(1)–O(5A) 2.342(3) Å] from a different bna, as well as three aqua ligands [Cd(1)–O 2.290(4)–2.388(3) Å]. The bna ligands here exhibit the monodentate-bidentate coordination mode (Scheme 1a), and the dihedral angle between the pair of naphthyl rings of the ligand is 73.6°. The oxygen atoms of aqua ligands form donor hydrogen bonds with the carboxylate or hydroxyl oxygen atoms [O⋯O 2.742(5)–2.936(5) Å] of bna from adjacent molecules, furnishing one-dimensional hydrogen-bonded chains running along the c -axis direction. Significant C–H⋯ π interactions²⁶ between the aromatic carboxylates

from adjacent chains are observed, since the edge-to-face separations of the adjacent aromatic rings are ca. 3.87 Å, resulting in two-dimensional supramolecular arrays containing micropores (Figure 2b). Although the area is ca. 6 Å × 6 Å in each square structure, the real volume of the cavity is further reduced due to the significant offset stacking of adjacent dimers.

The structure of **3** features two-dimensional coordination layers with unprecedented $[\text{Cd}_8(\mu_3\text{-OH})_2(\mu\text{-OH})_2(\mu\text{-H}_2\text{O})_2]^{12+}$ octanuclear metallacrown cores, in which four crystallographically independent Cd(II) atoms exhibit two different coordination geometries. To our best knowledge, only a few $[\text{Cd}_3(\mu_3\text{-OH})]^{5+}$ cores⁵ and octanuclear cadmium clusters²⁷ have been reported, and such an octanuclear metallacrown core featuring cadmium–hydroxy clusters has never been shown before this work. As depicted in Figure 3, each $\mu_3\text{-OH}$ interlinks the Cd(2), Cd(3), and Cd(4) atoms [Cd–O(1H) 2.177(3)–2.340(3) Å], with the nonbonding Cd···Cd distance of 3.650(2)–3.825(3) Å, and each $\mu\text{-OH}$ bridges the Cd(1) and Cd(3) atoms [Cd–O(2H) 2.272(4) and 2.276(4) Å] with the metal–metal separation of 3.682(3) Å. The Cd(1) and Cd(2) atoms, separated at 3.722(3) Å, are bridged by a $\mu\text{-aquo}$ oxygen atom [Cd–O(1W) 2.314(4) and 2.357(4) Å]. It should be noted that a very strong hydrogen bond [O(1W)···O(2HC) 2.448(5) Å] between adjacent $\mu\text{-aquo}$ and $\mu\text{-hydroxyl}$ oxygen atoms probably serves to consolidate the structure further. Moreover, three crystallographically independent bna ligands have been identified, and each acts in the bis-bidentate fashion [Cd–O 2.182(4)–2.353(4) Å] with the dihedral angle of 74.1°, 78.4°, or 87.6° (Scheme 1b). As such, the six-coordinate Cd(1) atom adopts a distorted octahedral geometry, and five-coordinate Cd(2) atom exhibits a trigonal-bipyramid geometry. For Cd(3) and Cd(4) atoms, each of them is further ligated to the aqua oxygen atoms [Cd–O 2.301(5)–2.404(7) Å] to complete a distorted octahedron geometry. Moreover, adjacent $[\text{Cd}_8(\mu_3\text{-OH})_2(\mu\text{-OH})_2(\mu\text{-H}_2\text{O})_2]^{12+}$ octanuclear metallacrown cores are inter-linked through the bis-bidentate bna ligand to form two-dimensional layers featuring cylindrical channels with an effective diameter of ca. 5.0 Å.²⁸ The free dimensions of these channels occupy 13.7% of the crystal volume;²⁹ a large number of lattice water molecules are located in them and are hydrogen-bonded to each other and to carboxylate or hydroxyl oxygen atoms of the host network [O···O 2.51(7)–3.122(7) Å]. The two-dimensional layers are extended into a three-dimensional supramolecular array via significant C–H··· π interactions between the aromatic rings from adjacent layers with the edge-to-face separations of 3.59–3.97 Å.

As illustrated in Figure 4, **4** consists of the two-

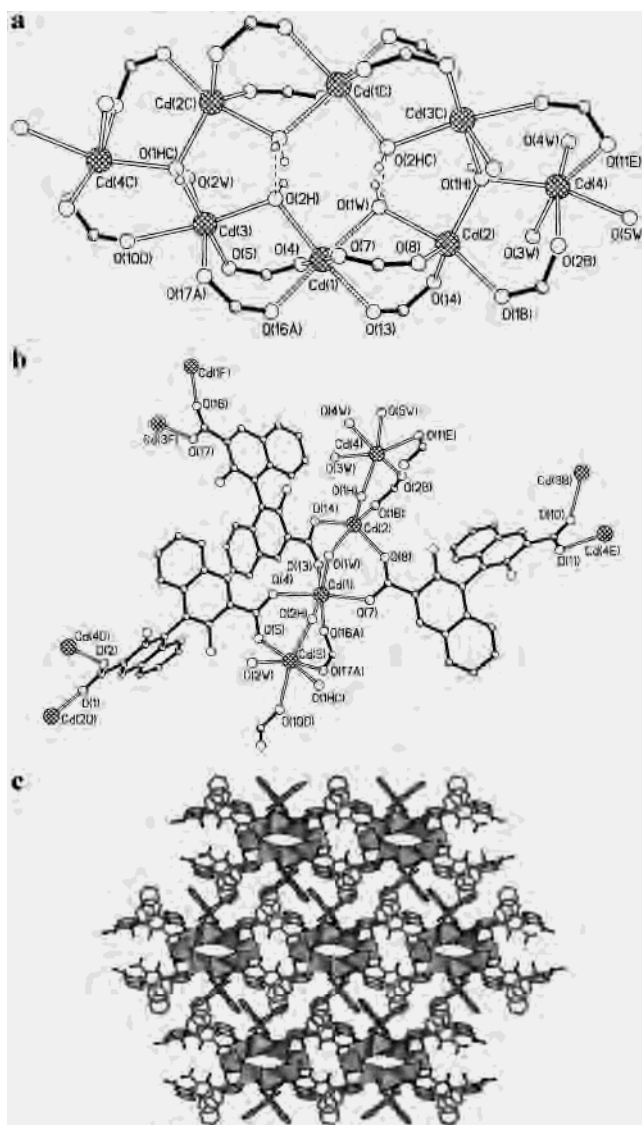


Figure 3. Perspective views showing the $[\text{Cd}_8(\mu_3\text{-OH})_2(\mu\text{-OH})_2(\mu\text{-H}_2\text{O})_2]^{12+}$ octanuclear metallacrown core (a), the coordination environments of the metal atoms (b), and three-dimensional network viewed along the a -axis direction (c) in **3**. The solvent molecules are omitted for clarity.

dimensional layers with $[\text{Zn}_4(\mu_3\text{-OH})_2]^{6+}$ clusters whose two crystallographically independent Zn(II) atoms adopt different coordination geometries. Each Zn(1) atom adopts a distorted octahedral geometry, being coordinated by four carboxylate oxygen atoms [Zn(1)–O 2.097(5)–2.197(5) Å] from four different bna ligands, a $\mu_3\text{-hydroxyl}$ oxygen atom [Zn(1)–O(1H) 2.077(4) Å], and an aqua ligand [Zn(1)–O(1W) 2.208(6) Å]. The Zn(2) atom is ligated to three different carboxylate oxygen atoms [Zn(2)–O 1.981(4)–2.128(5) Å] and two $\mu_3\text{-hydroxyl}$ oxygen atoms [Zn(1)–O 2.020(5) and 2.182(5) Å] in a distorted trigonal-bipyramidal geometry. Each $\mu_3\text{-OH}$ interlinks one Zn(1) atom and two Zn(2) atoms with the nonbonding Zn···Zn distances of 3.203(1) and 3.295(2) Å. Of the two crystallographically independent bna ligands, one acts in a bis-bidentate fashion (Scheme 1b) (dihedral angle of 96.1° between its naphthyl rings) whereas the other functions in a monodentate–bidentate fashion (Scheme 1c) (dihedral angle = 96.3°). The interactions give rise to two-dimensional coordination layers having butterfly-shaped $[\text{Zn}_4\text{-}$

(26) Janiak, C. *J. Chem. Soc., Dalton Trans.* **2000**, 3885–3896.

(27) (a) Saalfrank, R. W.; Burak, R.; Reihls, S.; Löw, N.; Hampel, F.; Stachel, H.-D.; Lentmaier, J.; Peters, K.; Perters, E.-M.; Schnering, H. G. *Angew. Chem., Int. Ed. Engl.* **1995**, *34*, 993–995. (b) Saalfrank, R. W.; Löw, N.; Trummer, S.; Sheldrick, G. M.; Teichert, M.; Stalke, D. *Eur. J. Inorg. Chem.* **1998**, 559–563.

(28) The channel dimensions are estimated from the van der Waals radii for carbon (1.70 Å), nitrogen (1.55 Å), oxygen (1.40 Å).

(29) Spek, A. L. *PLATON, A Multipurpose Crystallographic Tool*; Utrecht University: Utrecht, The Netherlands, 1999.

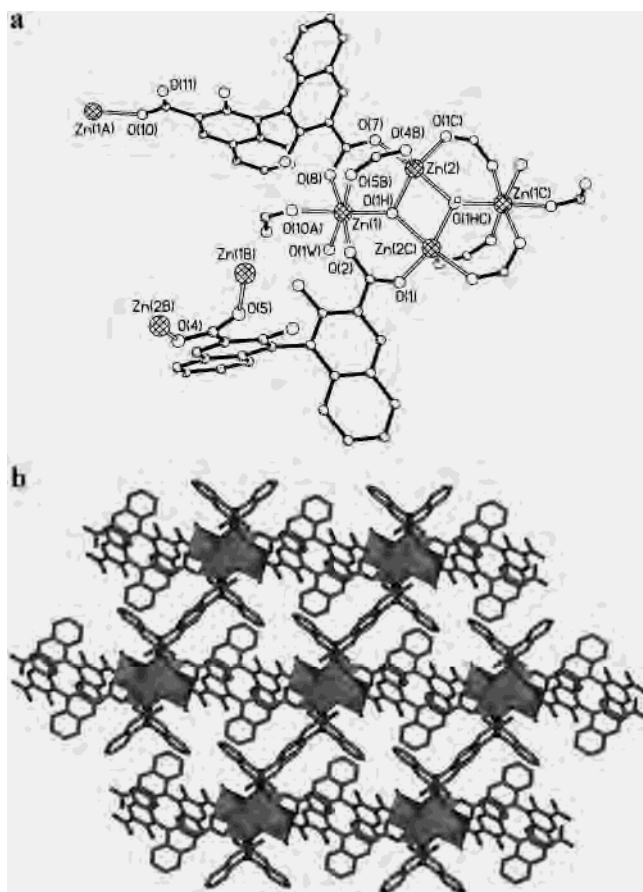


Figure 4. Perspective views showing the coordination environments of the metal atoms (a) and three-dimensional network viewed along the *a*-axis direction (b) in **4**. The solvent molecules and the pyridinium cations are omitted for clarity.

$(\mu_3\text{-OH})_2]^{6+}$ clusters constructed. These layers are further extended into a three-dimensional supramolecular array through $\text{C-H}\cdots\pi$ interactions between the aromatic rings from adjacent layers with the edge-to-face distance of ca. 3.76 Å. Clathrated between the layers are the lattice water, acetonitrile molecules, and pyridinium cations.

Luminescent Properties. The free H_2bna ligand displays very weak luminescence in the solid state at ambient temperature (see Figure S1 in the Supporting Information);¹¹ however, its complexes, **2** and **3**, exhibit intense greenish-blue radiation emission maxima at ca. 523 and 506 nm upon excitation at 355 nm, respectively. Complex **4** exhibits intense pure blue photoluminescence with an emission maximum at ca. 480 nm upon excitation at 355 nm (Figure 5). Similar to that found in its silver(I) complex,¹¹ the enhancement of luminescence in d^{10} complexes may be attributed to the chelation of the ligand to the metal center. This enhances the “rigidity” of the ligand and thus reduces the loss of energy through a radiationless pathway.^{11,12,30} Despite the different geometries and ligand environments of these complexes, the excitation spectra of **2–4** resemble each other in the peak profiles. They are also similar to that of

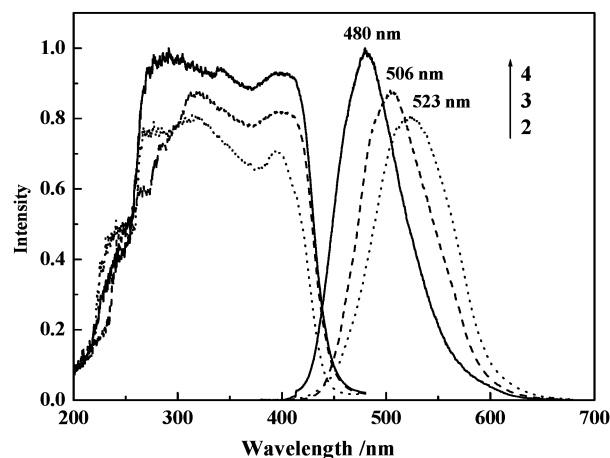
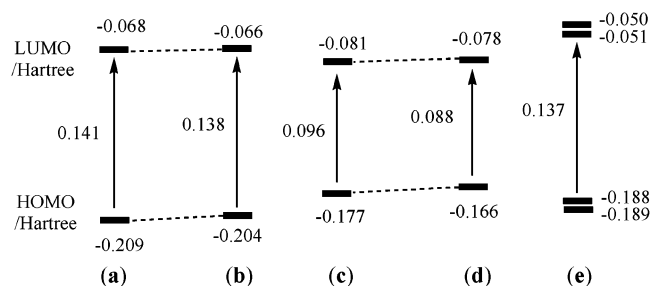


Figure 5. Photoluminescent spectra of **2–4** in solid state at room temperature.

Scheme 2. The HOMO, LUMO, and HOMO–LUMO Gaps for Hna (a), H_2bna (b), $\text{Cd}(\text{na})_2(\text{H}_2\text{O})_3$ (c), $\text{Cd}_2(\text{bna})_2(\text{H}_2\text{O})_6$ (d), and $[\text{Cd}_8(\text{OH})_4(\text{H}_2\text{O})_{10}(\text{na})_{12}]$ (e)



the free Hna ligand (see Figure S2 in the Supporting Information); i.e., these complexes, as well as Hna, all absorb the luminous energy through their naphthalene rings.^{11,12,30}

It was suggested that the luminescent properties of the substituted binaphthalenes are similar to those of the relevant substituted naphthalenes.¹² The MO calculations of the neutral H_2bna and its relevant substituted naphthalene (Hna), as well as the $\text{Cd}(\text{II})$ complexes (**2** and the hypothetical mononuclear $\text{Cd}(\text{na})_2(\text{H}_2\text{O})_3$), based on the experimental geometries,³¹ have been carried out for further verification. The contour plots (see Figure S3 in the Supporting Information) of the relevant HOMOs and LUMOs³² for Hna and H_2bna , together with the orbital energies, show high similarity. For the neutral ligands, both HOMOs are associated with the π -bonding orbital from the naphthalene rings, while LUMOs are mainly associated with the π^* -antibonding orbital from the naphthalene rings. In fact, the HOMO–LUMO gap for Hna (0.141 Hartree) is favorably compared with that of H_2bna (0.138 Hartree) (Scheme 2). For their $\text{Cd}(\text{II})$ complexes, both HOMOs are associated with the π -bonding orbital from the naphthalene rings, while LUMOs are mainly associated with Cd-O (from the carboxylate group) σ^* -antibonding orbital, localized more on the metal centers (Figure 6 and Figure S3 in the Supporting Information). The HOMO–LUMO gap for $\text{Cd}(\text{na})_2(\text{H}_2\text{O})_3$ (0.096 Hartree) is also favorably compared with $\text{Cd}_2(\text{bna})_2(\text{H}_2\text{O})_6$

(30) (a) Adamson, A. W.; Fleischauer, P. D. *Concepts of Inorganic Photochemistry*; John Wiley & Sons: New York, 1975. (b) *Photochemistry and Photophysics of Coordination Compounds*; Yersin, H., Vogler, A., Eds.; Springer-Verlag: Berlin, 1987.

(31) Gupta, M. P.; Dutta, B. P. *Cryst. Struct. Commun.* **1975**, *4*, 37–38.

(32) HOMO, highest occupied molecular orbital; LUMO, lowest unoccupied molecular orbital.

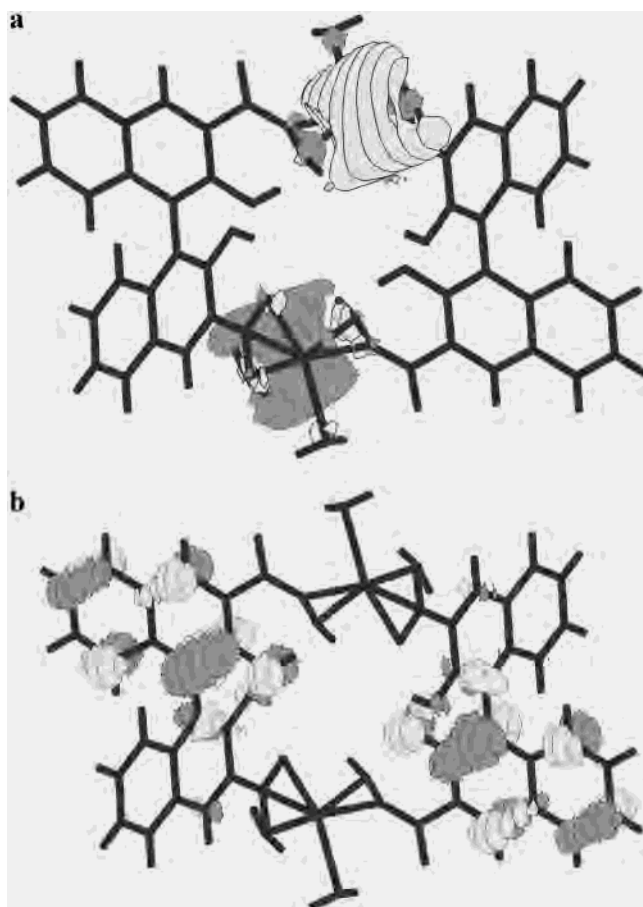


Figure 6. The contour plots of the relevant LUMOs (a) and HOMOs (b) for **2**.

(0.088 Hartree). It should be pointed out that the carboxylate group would be more negatively charged owing to the weak electron acceptor nature of Cd(II) so that the energy of HOMO is significantly raised compared to that of carboxylic acid. The significant reduction in the HOMO–LUMO gap can be seen for the Cd(II) complexes compared with the neutral ligand, which is similar to the result found in our recent report on a class of d^{10} metal complexes with ophen (Hophen = 1*H*-[1,10]phenanthroline-2-one).¹³ Although there are deviations (the maximum deviation (0.040 Hartree) is found for Hna) between the HOMO–LUMO as obtained by computations and by experiment, this is justified as only the ground states were taken into consideration in the calculations. Moreover, the transverse interactions, such as the π – π stacking, C–H \cdots π interactions, and hydrogen-bonding interactions, all of which must exist in the real solid state, are expected to play an essential role in decreasing the HOMO–LUMO gaps.^{12,13,30,33} It can be concluded from the MO calculations that, for the free ligands, their luminescence can be assigned to the $\pi_L \rightarrow \pi_L^*$ transition, whereas for the metal complexes, their luminescence can be assigned to $\pi_L \rightarrow 5s$ ligand-to-metal charge transfer (LMCT).^{12,34} Additionally, the photoluminescence mechanisms of the

complexes based on bna are reliably similar to those of the analogous complexes with na¹² despite the minor differences between the values of the gaps of the two ligands or their coordination complexes.

The above results encouraged us to further carry out MO calculations of a hypothetical $[\text{Cd}_8(\text{OH})_4(\text{H}_2\text{O})_{10}(\text{na})_{12}]$ which has the metallacrown core of authentic $[\text{Cd}_8(\text{OH})_4(\text{H}_2\text{O})_{10}(\text{bna})_6]$ in **3**. The calculations reveal that the HOMO is associated with the π -bonding orbital from the naphthalene rings whereas the LUMO is mainly associated with Cd–O (from the carboxylate group, the aqua, and hydroxyl oxygen atoms) σ^* -antibonding orbital, which is localized more on the metal centers, and the HOMO–LUMO gap is 0.137 Hartree (Scheme 2e). Compared with that of $\text{Cd}(\text{na})_2(\text{H}_2\text{O})_3$, a larger HOMO–LUMO gap here was calculated, which may be attributed to the rigid $[\text{Cd}_3(\mu_3\text{-OH})]^{5+}$ cores in $[\text{Cd}_8(\text{OH})_4(\text{H}_2\text{O})_{10}(\text{na})_{12}]$.¹³ The above result implies that the photoluminescence of **3** can be attributed to the $\pi_L \rightarrow 5s$ transition (LMCT), so that our previous speculation of the LMCT mechanisms for the Zn(II) or Cd(II) cluster-based coordination polymers with aromatic carboxylate ligands are possibly correct.⁶

Similar to the lifetime of $[\text{Zn}_4\text{O}(\text{OAc})_6]$ (10 ns),⁷ the lifetimes of **3** and **4** are ca. 20 and 15 ns, respectively, being significant longer than those of the other compounds (0.69 ns for **1** and 2.02 ns for **2**). This fact may be ascribed to the presence of the metal clusters, since the $\mu_3\text{-OH}$ ligand may also tighten the whole framework, resulting in the weaker vibrations. A similar behavior was also observed for the monomeric and multinuclear d^{10} compounds with ophen;¹³ the metal–hydroxy (or oxy) clusters also have significantly longer emission lifetimes than those without metal–hydroxy (or oxy) clusters. The emission bands of the metal complexes in this work, whether they arise from metal–hydroxy clusters or otherwise, can be assigned to the LMCT emission.^{6,7,9,34}

From the theoretical viewpoint, because of the impact of relativistic effect, the coordination structures, and electron correlation effects, the $(n+1)s$ orbitals of d^{10} metal are contracted and hereby have lower energy.^{34,35,36} Common Zn(II) or Cd(II) coordination complexes without metal–hydroxy (or oxy) clusters (such as **2**) may also possess LMCT photoluminescent property.^{9,34} On the other hand, HOMOs or LUMOs, in fact, are associated with the orbitals from the metal center and/or the ligands.^{12,34} For the Zn(II) or Cd(II) metal–hydroxy (or oxy) clusters, coordination complexes with alkyl or aromatic carboxylate ligands^{6,7} (such as this work), the emission bands can be assigned to the LMCT emission. However, if the ligand is a heterocyclic

(33) (a) Cassoux, P. *Science* **2001**, *291*, 263–264. (b) Tanaka, H.; Okano, Y.; Kobayashi, H.; Suzuki, W.; Kobayashi, A. *Science* **2001**, *291*, 285–287. (c) Kobayashi, A.; Tanaka, H.; Kobayashi, H. *J. Mater. Chem.* **2001**, *11*, 2078–2088. (d) Zheng, S.-L.; Zhang, J.-P.; Wong, W.-T.; Chen, X.-M. *J. Am. Chem. Soc.* **2003**, *125*, 6882–6883.

(34) (a) Blasse, G.; Bleijenberg, K. C.; Powell, R. C. *Structure and Bonding* **42: Luminescence and Energy Transfer**; Springer-Verlag: Berlin, 1980. (b) Crosby, G. A.; Highland, R. G.; Truesdell, K. A. *Coord. Chem. Rev.* **1985**, *64*, 41–53. (c) Kutal, C. *Coord. Chem. Rev.* **1990**, *99*, 213–252. (d) Blasse, G.; König, E.; Padhye, S. B.; Sonawane, P. B.; West, D. X. *Structure and Bonding*, **76: Complex Chemistry**; Springer-Verlag: Berlin, 1991.

(35) Balasubramanian, K. *Relativistic Effects in Chemistry. Part A: Theory and Techniques; Part B: Applications*; Wiley: New York, 1997.

(36) (a) Pykkö, P. *Chem. Rev.* **1988**, *88*, 563–594. (b) Kaltsoyannis, N. *J. Chem. Soc., Dalton Trans.* **1997**, 1–12. (c) Pykkö, P. *Chem. Rev.* **1997**, *97*, 597–636. (d) Yam, V. W. W.; Lo, K. K. W. *Chem. Soc. Rev.* **1999**, *28*, 323–334.

aromatic ligand, such as ophen in our previous report,¹³ in which the heteroatoms can effectively decrease the π and π^* orbital energies, the HOMO and LUMO, as well as the orbitals with energies close to the HOMO and LUMO, may be not significantly contributed by the metal atoms, so that LMCT can be excluded from consideration;^{13,35} i.e., the Zn(II) or Cd(II) metal–hydroxy (or oxy) cluster coordination complexes with the heterocyclic aromatic ligands probably will not exhibit LMCT photoluminescence activity.

Conclusions

The H₂bna ligand, in which the two twisted naphthyl rings are connected by a single C–C bond, forms a dimeric Cd(II) complex and two new d¹⁰ metal–hydroxy cluster-based coordination polymers, which display uncommon structural features and useful photoluminescent activity in the blue/green region. The photoluminescence, as probed by MO calculations, arises from LMCT emissions. The report,

which adopts a new approach for the study of the photoluminescent properties of metal-cluster-based coordination polymers by using model compounds, reveals first that the structure of the ligand has much more important effect than the d¹⁰ metal–hydroxy (or oxy) cluster in photoluminescence, and second that the presence of the d¹⁰ metal–hydroxy (or oxy) cluster can significantly increase the emission lifetime.

Acknowledgment. The authors thank Dr. Zhen-Yang Lin (Department of Chemistry, The Hong Kong University of Science and Technology) and Dr. Seik Weng Ng (University of Malaya) for helpful discussions. This work was supported by the National Natural Science Foundation of China (No. 20001008), Ministry of Education of China (No. 01134).

Supporting Information Available: Additional figures and tables. Crystallographic data in CIF format. This material is available free of charge via the Internet at <http://pubs.acs.org>.

IC034847I